On the influence of polarization effects in predicting the interfacial structure and capacitance of graphene-like electrodes in ionic liquids

Eunsu Paek, Alexander J. Pak, and Gyeong S. Hwang

Citation: The Journal of Chemical Physics **142**, 024701 (2015); doi: 10.1063/1.4905328
View online: http://dx.doi.org/10.1063/1.4905328
View Table of Contents: http://scitation.aip.org/content/aip/journal/jcp/142/2?ver=pdfcov
Published by the AIP Publishing

On the influence of polarization effects in predicting the interfacial structure and capacitance of graphene-like electrodes in ionic liquids

Eunsu Paek,[a] Alexander J. Pak,[a] and Gyeong S. Hwang[b]
McKetta Department of Chemical Engineering, University of Texas, Austin, Texas 78712, USA

(Received 5 September 2014; accepted 19 December 2014; published online 8 January 2015)

The electric double layer (C_D) and electrode quantum (C_Q) capacitances of graphene-based supercapacitors are investigated using a combined molecular dynamics and density functional theory approach. In particular, we compare an approach that includes electronic polarization to one that is polarization-free by evaluating both C_D and C_Q using [EMIM][BF_4] ionic liquid as a model electrolyte. Our results indicate that the inclusion of polarization effects can yield higher C_D values—in this study by up to 40% around ±2 V—which we attribute primarily to the presence of charge smearing at the electrode-electrolyte interface. On the other hand, we find that the polarization-induced distortion of the electronic structure of graphene does not noticeably alter the predicted C_Q. Our analysis suggests that an accurate description of the spatial charge distribution at the graphene interface due to polarization is necessary to improve our predictive capabilities, though more notably for C_D. However, the conventional polarization-free approximation can serve as an efficient tool to study trends associated with both the C_Q and C_D at the interface of various graphene-like materials. © *2015 AIP Publishing LLC*. [http://dx.doi.org/10.1063/1.4905328]

I. INTRODUCTION

Electrochemical double layer capacitors (EDLCs), or supercapacitors, are a class of energy storage devices known for their large power densities and long lifetimes.[1,2] As such, supercapacitors have become increasingly favored for use in high-power applications such as hybrid or electric vehicles, communications, load-leveling, back-up power systems, and portable electronics.[3,4] However, the wide-spread utilization of supercapacitors has been stagnated by their limited energy density. Within the last several years, researchers have proposed graphene-based materials and ionic liquids (IL) as candidates for the electrode and electrolyte, respectively.[5–9] Based on these two materials, many efforts have been dedicated towards discovering the underlying mechanisms at the electrode-electrolyte interface in order to develop design strategies to improve the energy density.

Advances in computational capabilities have propelled the use of molecular simulation towards understanding the atomistic phenomena at the electrode-electrolyte interface. In particular, classical molecular dynamics (CMD) has been commonly used to study the electric double layer capacitance and microstructure of various graphitic-IL interfaces.[10–16] The CMD method relies on the careful selection of force fields that can emulate the interatomic interactions of the electrolyte and electrode. In the past, non-polarizable force field frameworks, as implemented in CHARMM,[17] AMBER,[18] and OPLS,[19] have been popular options due to their simplicity and inexpensive computational burden, which can be further reduced with the adoption of coarse-grained approaches, and are often re-parameterized for each IL pair studied. In order to predict the microstructure of the EDL using these force fields, it is especially important to accurately describe the electrostatic interactions. The simplest and most prevalent approach is to assign fixed partial charges to each atom; in the case of metallic electrodes, excess charge is distributed uniformly or held at the so-called constant charge condition.

Recently, the validity of the constant charge condition has been questioned by several researchers. Merlet and coworkers demonstrated that by allowing the fluctuation of the partial atomic charges, according to the variational principle (the so-called constant potential condition), the predicted EDL microstructure was slightly perturbed; the computed EDL capacitances, however, were in good agreement with results from constant charge simulations.[20] Vatamanu and coworkers have also shown that the same constant potential treatment can be used to accurately predict double-layer relaxation times.[21] Here, we should note that the electrode atoms were modeled as Gaussian charge distributions which may not account for the true electric polarizability due to its inherent symmetry. In addition, the electrolyte atoms were kept as fixed point charges throughout the simulations. As such, a comprehensive study on the influence of electric polarizability in predicting the EDL capacitance is currently lacking.

Beyond the EDL capacitance, several theoretical studies have indicated that the electrode quantum capacitance is also an important contributor to the overall capacitance of graphene-based supercapacitors.[22–27] The quantum capacitance is related to the electronic density of states (DOS), which can be evaluated using quantum mechanical calculations. Prior efforts have typically evaluated the DOS of the electrode in the absence of the electrolyte. However, it is still unclear

[a]E. Paek and A. J. Pak contributed equally to this work.
[b]Author to whom correspondence should be addressed. Electronic mail: gshwang@che.utexas.edu; Telephone: 512-471-4847.

the extent to which interactions with the electrolyte may modify the electronic structure and subsequently, the quantum capacitance.

In this work, we investigate the efficacy of classical methods which exclude electronic polarization effects in the computation of the total interfacial capacitance, which depend upon the EDL and quantum capacitances, using [EMIM][BF_4] and graphene as a model system. First, we compare the spatial charge distribution and EDL capacitances as calculated using classical force fields and density functional theory (DFT), the latter of which inherently considers electronic polarization. We then compare the calculated DOS and quantum capacitance of graphene in the presence and absence of [EMIM][BF_4]. Our results demonstrate that the predicted interfacial capacitance can be sensitive to polarization effects primarily due to differences in the estimated C_D.

II. COMPUTATIONAL DETAILS

A. Classical Molecular Dynamics

We employed CMD simulations with the all-atom OPLS force field[19,28] to determine the microstructure of [EMIM][BF_4] near the graphene electrode, using the Large-Scale Atomic/Molecular Massively Parallel Simulator (LAMMPS) program.[29] As illustrated in Fig. 1, our simulation cell consisted of 15 [EMIM][BF_4] ion pairs in contact with a graphene electrode; the dimensions of the system were $12.816 \times 12.332 \times 50$ Å^3, corresponding to 60 C atoms in the electrode, and were periodic only in the x and y directions. For charged systems of $\sigma = \pm 10.14$ μC/cm^2, we assigned equally distributed excess charge to the C atoms in graphene; an extra counterion was added to the electrolyte to maintain charge neutrality. The position of each atom in graphene was held fixed throughout the simulations.

We ran CMD at 700 K for 2 ns, followed by 3 ns at 313 K to equilibrate the system, which we find to be sufficiently long to achieve thermal equilibrium (Figure S1).[30] After equilibration, the final configurations were used to continue a 1.5 ps production run using both CMD and *ab-initio* MD (AIMD, as described below); this is sufficiently long to gather statistics from thermal fluctuations without greatly perturbing the microstructure. All simulations were run in the NVT ensemble with the temperature controlled by a Nose-Hoover thermostat[31] with a time step of 1 fs. Spherical cutoffs of 10 Å and 12 Å were used for the Lennard-Jones (LJ) and Coulomb interactions, respectively. Electrostatic interactions beyond the cutoff were calculated using the Ewald summation method; the inter-slab interactions in the z direction were removed by inserting a large vacuum space outside of the graphene sheets.[32,33] We employed the force field (FF) parameters for EMIM and BF_4 from Refs. 34 and 35, respectively, while the LJ parameters of graphene were from Ref. 36. All MD results reported herein were obtained from the average of 30 independent simulations with different initial atomic configurations.

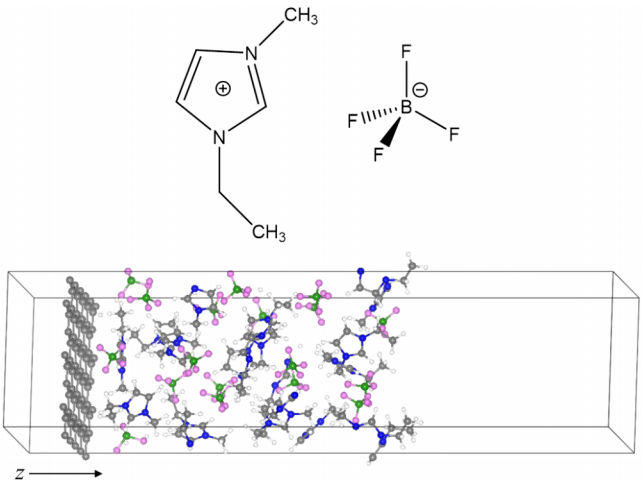

FIG. 1. Schematic of EMIM, BF_4, and the simulation domain containing a graphene sheet and 15 [EMIM][BF_4] ion pairs. Each C/N/H (graphene and EMIM) and B/F (BF_4) atom is depicted by grey/blue/white and green/pink balls, respectively.

B. Density Functional Theory

We performed AIMD simulations for 1.5 ps at 313 K within the Born-Oppenheimer approximation using the equilibrated configurations from CMD (see above) as initial atomic positions. Geometric optimization was performed before each AIMD simulation to ensure that all forces were minimized below a tolerance of 0.02 eV/Å. The potential energy surfaces were generated using DFT within the Perdew-Berke-Ernzerhof generalized gradient approximation[37] with dispersion corrections from the Grimme method (DFT-D2),[38] as implemented in the Vienna *Ab-initio* Simulation Package[39] (VASP) using only the Γ point. The projector augmented wave method with a planewave basis set was employed to describe the interaction between the core and valence electrons. An energy cutoff of 350 eV was applied during the AIMD simulations. The final configurations were used to perform single-point electronic structure calculations with an increased energy cutoff of 400 eV and $6 \times 6 \times 1$ Γ-centered Monkhorst-Pack[40] k-point mesh.

III. RESULTS AND DISCUSSION

The total interfacial capacitance (C_T) depends upon the electrode quantum capacitance (C_Q) and electric double layer capacitance (C_D) which are in series (i.e., $1/C_T = 1/C_Q + 1/C_D$). In fact it is known that for supercapacitors with graphene-like electrodes, C_Q and C_D can be of comparable magnitudes; it is therefore critical to accurately estimate both capacitances. In Secs. III A and III B, we compare the extent to which the inclusion of electronic polarizability influences both the predicted C_Q and C_D of graphene immersed in [EMIM][BF_4] ionic liquid.

A. Microstructure and electric double layer capacitance

In the literature, C_D is often reported using either its differential ($d\sigma/d\phi_D$) or integral ($\sigma/[\phi_D\text{-}\phi_Z]$) forms, where

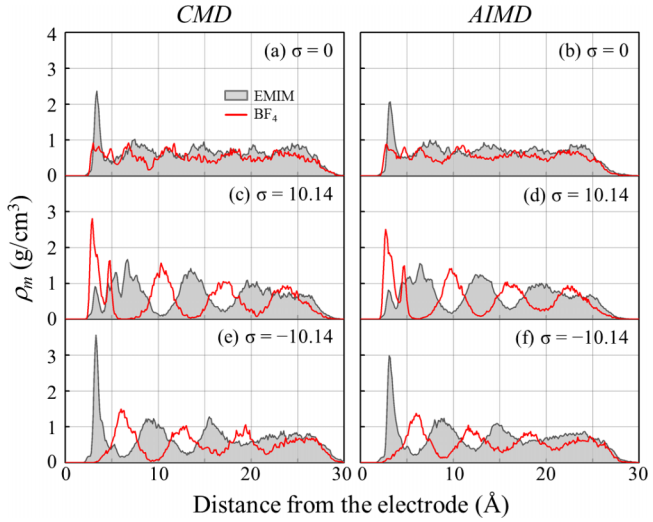

FIG. 2. Mass density (ρ_m) profiles for EMIM and BF_4 in the direction normal to graphene using classical (CMD, left) and *ab-initio* (AIMD, right) molecular dynamics at the listed excess surface charge densities (σ in $\mu C/cm^2$). Note that both EMIM and BF_4 profiles taper beyond 25 Å as our simulations are limited to a finite number of ion pairs.

σ is the excess electrode surface charge and ϕ_D (ϕ_Z) is the potential drop within the EDL (potential of zero charge). However, of the two, the integral C_D is more commonly reported as it directly indicates the total charge storage performance of a supercapacitor; as such, the integral C_D is also used in this work. In order to evaluate the C_D, we first determine ϕ_D at different σ from the charge density (ρ_q) distributions at the interface; our focus here is to isolate the influence of charge polarization on ρ_q with respect to a given IL ion arrangement. Therefore, in this section, we compare the ρ_m, ρ_q, and ϕ_D as determined using CMD and AIMD.

Figure 2 shows a comparison between the ρ_m of EMIM and BF_4 near graphene using CMD and AIMD. Near the uncharged electrode [Figs. 2(a) and 2(b)], it is evident that the predicted ρ_m profiles using CMD and AIMD are qualitatively similar. For example, both EMIM and BF_4 profiles exhibit a peak around 3–4 Å away from the electrode; this peak is especially distinct for EMIM, suggesting that the cation has a tendency to flatten and align parallel to the electrode due to van der Waals interactions, similarly to other imidazolium-based ILs.[10,22,41] Note that slight discrepancies between peak positions and broadness can be expected as a result of thermal fluctuations. Further away from the electrode, each of the EMIM and BF_4 profiles are relatively flat with nearly equal magnitude, as charge neutrality must be maintained,[22] with average density 1.24 and 1.29 g/cm^3 using CMD and AIMD, respectively, which is in good agreement with experimental values.[42]

When the electrodes are charged, the similarities between the predicted ρ_m profiles using CMD and AIMD persist. At $\sigma = 10.1\ \mu C/cm^2$ [Figs. 2(c) and 2(d)] and $\sigma = -10.1\ \mu C/cm^2$ [Figs. 2(e) and 2(f)], both simulation methods display a distinctly sharp counterion profile near the electrode while the coion profile is suppressed; this is due to electrostatic attraction (repulsion) of the counterions (coions) with the electrode. The accumulation of counterions at the electrode interface triggers the successive formation of layers that alternate between coions and counterions, as indicated by the offset oscillations of their respective ρ_m profiles, which is also observed for other IL pairs.[11,13,22] The distinct similarity between the microstructures predicted by the two CMD and AIMD methods suggests that the potential energy surface of the system is comparable enough to retain the same molecular configuration within 1.5 ps despite the inclusion of charge polarization when using AIMD. We have further tested the evolution of the microstructure over 6 ps at a larger temperature of 450 K (Figure S2), in which we find the EDL structure to be qualitatively similar although the IL layers are predicted to be less rigid in the AIMD case; additional discussion can be found in the supplementary material.

We next investigate the differences in ρ_q when using CMD and AIMD as shown in Figs. 3(a)–3(c). In the CMD case, ρ_q is computed based on the positions and partial charges of each atom (the electrode charge is not included). On the other hand, the ρ_q of the AIMD case is approximated based on the valence charge density differences.[43] Given the similarity between the microstructures, we are effectively investigating

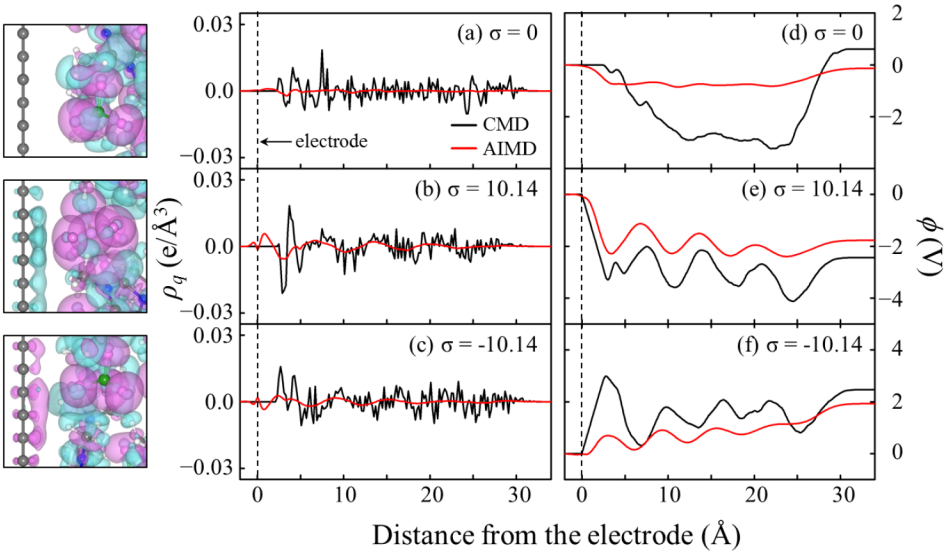

FIG. 3. Spatial charge density (ρ_q, middle) and potential variation (ϕ, right) profiles using classical (CMD, black) and *ab-initio* (AIMD, red) molecular dynamics at the listed excess surface charge densities (σ in $\mu C/cm^2$); here, the electrode surface potential is used as reference. The position of graphene is indicated by the dashed line. Band decomposed charge density isosurfaces (left) are also shown from one AIMD snapshot with blue and purple indicating positive and negative charge, respectively (at 0.0012 e/bohr^3).

the possible charge broadening due to polarization. We observe two stark differences between the two simulation techniques. First, ρ_q is constant and zero in the region between the electrode and electrolyte in the CMD case (within 3 Å of the electrode), whereas the AIMD profile exhibits shallow (substantial) charge fluctuation in the neutral (charged) cases. Second, the ρ_q profiles using CMD tend to be jagged and abruptly oscillate between positive and negative charge in contrast to the broadened and smoothly transitioning profiles using AIMD. Both of these observations can be attributed to the disparity in the treatment of charge—CMD simplifies the charge density using the aforementioned fixed point charge approximation while AIMD allows the spatial charge spreading through the use of a finely discretized grid; it is also possible that the limited sampling of microstates (the so-called sample size effect) can also partially account for the large variation seen in the CMD case. Additionally in the latter case, the π orbitals of graphene are polarized toward the IL ions [as seen from the band decomposed charge density isosurfaces from AIMD]; we note that this surface charge smearing towards the EDL should be appreciable in metallic electrodes.

From ρ_q, we subsequently solve for the spatial variation of ϕ by solving Poisson's equation ($\nabla^2\phi = -\rho_q/\varepsilon$, where ε is the vacuum permittivity). In the CMD case, we assume an implicit electric field strength at the electrode surface ($=\sigma/\varepsilon$);[22] in the AIMD case, however, no assumptions are necessary since the electrode charge is explicitly included in ρ_q. The resulting ϕ profiles are shown in Figs. 3(d)–3(f). From the uncharged case [Fig. 3(d)], the ϕ_Z is equivalent to the ϕ_D, which is the difference between the bulk IL potential (in this case, the ϕ far away from the electrode) and the electrode surface potential. Here, we find that the ϕ_Z calculated from CMD and AIMD are 0.15 V and −0.61 V, respectively. We should clarify, however, that these values are not necessarily physical and only demonstrate the differences in the predicted ϕ_Z. Due to sample size effects, more quantitative calculations would require more extensive sampling with either a larger simulation domain or length of time, which is currently a non-trivial challenge for AIMD and outside the scope of this work.

When the electrodes are charged [Figs. 3(e) and 3(f)], it can be seen that the computed ϕ_D is consistently lower in magnitude using AIMD compared to that of CMD; the ϕ_D is estimated to be 1.79 and 2.44 V at the cathode (or −1.90 and −2.47 V at the anode) using AIMD and CMD, respectively, when $\sigma = 10.1\ \mu C/cm^2$ ($=-10.1\ \mu C/cm^2$). This can be largely attributed to the variation of ϕ in the region (around 3 Å in thickness) between the electrode and electrolyte. Notably, the magnitude of ϕ tends to increase to a greater extent when using CMD; this suggests that the local electric field strength is overestimated when charge polarization effects are excluded; this attribute remains when the system is simulated at 450 K over 6 ps (Figure S3). However, we also observe that while the discrepancy in ϕ at the interface can be large, this discrepancy can be mitigated as evidenced near the anode. This is likely related to the fact that the effective screening of the electric field by the EDL ions is dependent upon the degree of counterion-coion segregation, which is comparatively less stringent near the anode; similar phenomena has been predicted for [BMIM][PF_6] near planar and curved electrodes.[25,26] Nonetheless, we emphasize that the EDL potential drop can be well-approximated by the variation up to the first IL layer (typically 1.0−1.5 nm thick), which can also be seen in previous studies of different IL systems.[44–46] Beyond the first IL layer, the IL ions tend to have less ionic ordering (analogous to the diffuse layer of Gouy-Chapman-Stern theory) as the electrode surface charge is sufficiently screened, thereby resulting in limited fluctuation of the potential. Hence, to determine C_D, it is most critical to describe the microstructure, and more importantly the spatial charge distribution, within the first IL layer.

We can now compare the integral C_D as estimated from the AIMD ($C_{D,AIMD}$) and CMD ($C_{D,CMD}$) simulations. At $\sigma = 10.1\ \mu C/cm^2$ and assuming $\phi_Z = 0$ V, $C_{D,AIMD} = 5.67\ \mu F/cm^2$, which is 36% greater than $C_{D,CMD} = 4.16\ \mu F/cm^2$; with the inclusion of ϕ_Z, which may range from −0.2 to 0.2 V, $C_{D,AIMD}$ is still larger than $C_{D,CMD}$ by 32%–40%. Similarly at $\sigma = -10.1\ \mu C/cm^2$, $C_{D,AIMD} = 5.32\ \mu F/cm^2$, which is 29% greater than $C_{D,CMD} = 4.11\ \mu F/cm^2$. These results indicate that the inclusion of polarization effects, such as through the use of AIMD, yields larger predicted values for C_D (although still within an order of magnitude). However, given the computational burden of such methods, the use of CMD can serve as an efficient means to evaluate the C_D of various graphene-like materials immersed in ILs relative to each other.

B. Electronic structure and quantum capacitance

The C_Q of a low-dimensional material such as graphene is defined by the following expression:[22,47]

$$C_Q = e^2 \int_{-\infty}^{+\infty} D(E) F_T(E-\mu) dE,$$

where D(E) is the electronic DOS, F_T is the thermal broadening function [$=(4k_BT)^{-1}\mathrm{sech}^2(E/2k_BT)$], e is the elementary charge, μ is the shift in the electrochemical potential, and E is the energy with respect to the Fermi level (E_F). As such, C_Q profiles tend to closely resemble that of their DOS after thermal broadening. In the case of pristine graphene, the valence and conduction bands exhibit conical band dispersion near the Dirac point which is reflected by the well-known symmetric and linear DOS near the charge neutrality point.[22,48] In Fig. 4(a), we show the DOS calculated for pristine graphene[49] (shaded region).

Figure 4(a) also depicts the total DOS of the graphene sheet immersed in [EMIM][BF_4] with the additional projected DOS for representative IL ions adjacent to graphene. It is evident that the DOS of the immersed graphene is nearly the same as that of free-standing graphene within $-2 < E - E_F < 2$ eV; the observed kinks indicate that interactions with adjacent ILs can slightly modify the electronic structure and thus the DOS. In addition, we find that the frontier molecular orbital peaks (i.e., highest occupied, HOMO and lowest unoccupied, LUMO) for EMIM and BF_4 are positioned beyond 2 eV from E_F, implying the unlikelihood of charge transfer between the electrode and electrolyte. These results suggest that the C_Q of graphene, which is proportional to the

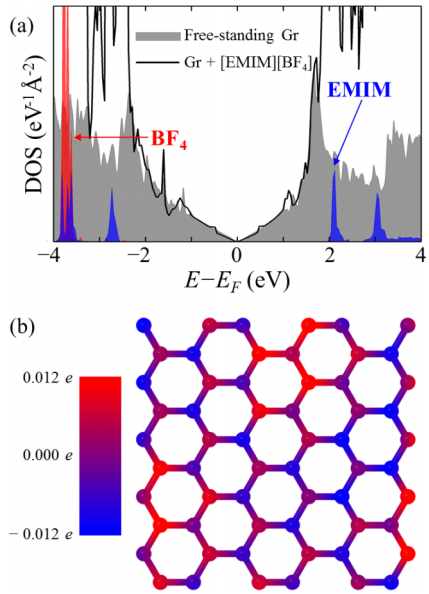

FIG. 4. (a) Calculated DOS of free-standing graphene (shaded) and graphene immersed in [EMIM][BF_4] ionic liquid (solid black). Corresponding projected DOS for EMIM and BF_4 are shown as the shaded blue and red regions, respectively. (b) Polarization-induced variation in the charge distribution along the graphene lattice calculated using Bader charge analysis. The DOS plot was obtained from the average of 4 randomly selected configurations.

DOS, is largely unaffected by the interactions with IL ions. On the other hand, the polarization by IL ions can pointedly alter the charge distribution along the graphene lattice. Figure 4(b) depicts the Bader charges when the electrode is uncharged. Noticeable electronic inhomogeneity (or so-called charge puddles) is observed in which the charge of any given C atom fluctuates between −0.012 and 0.012 e. Such charge puddles may serve as scattering sites and can considerably suppress electronic conductivity.[50,51] Nonetheless, as the effect of electronic polarizability on the DOS is insignificant, our findings suggest that the C_Q calculated without the consideration of polarization is sufficiently representative of graphene-like materials immersed in ILs.

IV. SUMMARY

We have investigated the sensitivity of the predicted electric double layer (C_D) and electrode quantum (C_Q) capacitances of graphene-based supercapacitors to the inclusion of electronic polarization effects. To evaluate the C_D, we performed CMD and AIMD with graphene using [EMIM][BF_4] IL as a model electrolyte. Our results indicate that given similar microstructures of the electric double layer, the spatial charge distributions tend to be broader and smoother in the AIMD case as compared to the CMD case. Notably, the smearing of the graphene π electrons toward the ionic liquid is well-represented using AIMD, which subsequently results in up to a 40% increase in C_D around ±2 V. To evaluate the C_Q, we performed density functional theory calculations to compute the electronic DOS of graphene with and without neighboring IL ions. Our analysis reveals that the IL interactions do not noticeably affect the C_Q as the DOS is only slightly perturbed and charge transfer between the electrode and electrolyte is unlikely. However, we found that the polarization by ILs induces charge redistribution along graphene, which can be an important consideration for other properties such as electrical conductivity.

Therefore, is it necessary to include polarization effects to predict the capacitance of graphene-based supercapacitors in ILs? Our study suggests that the biggest hurdle is to accurately and easily emulate the surface charge polarization in metallic electrodes. Nonetheless, before less computational burdensome approaches are developed, polarization-free methods remain an efficient means to comparatively evaluate the capacitance of different graphene-like materials immersed in ILs.

ACKNOWLEDGMENTS

This work was partially supported by the Welch Foundation (F-1535) and the Korea CCS R&D Center (KCRC) grant (No. 2014M1A8A1049270) funded by the Korea Government (Ministry of Science, ICT and Future Planning). We would also like to thank the Texas Advanced Computing Center for use of the Stampede supercomputing system (OCI-1134872).

[1]B. E. Conway, *Electrochemical Supercapacitors: Scientific Fundamentals and Technological Applications* (Kluwar Academic, New York, 1999).
[2]G. Wang, L. Zhang, and J. Zhang, Chem. Soc. Rev. **41**, 797 (2012).
[3]P. F. Ribeiro, B. K. Johnson, M. L. Crow, A. Arsoy, and Y. Liu, Proc. IEEE **89**, 1744 (2001).
[4]I. Hadjipaschalis, A. Poullikkas, and V. Efthimiou, Renewable Sustainable Energy Rev. **13**, 1513 (2009).
[5]P. Simon and Y. Gogotsi, Acc. Chem. Res. **46**, 1094 (2013).
[6]M. Armand, F. Endres, D. R. MacFarlane, H. Ohno, and B. Scrosati, Nat. Mater. **8**, 621 (2009).
[7]H. Liu, Y. Liu, and J. Li, Phys. Chem. Chem. Phys. **12**, 1685 (2010).
[8]G. Xiong, C. Meng, R. G. Reifenberger, P. P. Irazoqui, and T. S. Fisher, Electroanalysis **26**, 30 (2014).
[9]F. Béguin, V. Presser, A. Balducci, and E. Frackowiak, Adv. Mater. **26**, 2219 (2014).
[10]S. Maolin, Z. Fuchun, W. Guozhong, F. Haiping, W. Chunlei, C. Shimou, Z. Yi, and H. Jun, J. Chem. Phys. **128**, 134504 (2008).
[11]J. Vatamanu, L. Cao, O. Borodin, D. Bedrov, and G. D. Smith, J. Phys. Chem. Lett. **2**, 2267 (2011).
[12]G. Feng, J. S. Zhang, and R. Qiao, J. Phys. Chem. C **113**, 4549 (2009).
[13]S. A. Kislenko, I. S. Samoylov, and R. H. Amirov, Phys. Chem. Chem. Phys. **11**, 5584 (2009).
[14]J. Vatamanu, Z. Hu, D. Bedrov, C. Perez, and Y. Gogotsi, J. Phys. Chem. Lett. **4**, 2829 (2013).
[15]C. Merlet, B. Rotenberg, P. A. Madden, P.-L. Taberna, P. Simon, Y. Gogotsi, and M. Salanne, Nat. Mater. **11**, 306 (2012).
[16]Y. Shim, H. J. Kim, and Y. Jung, Faraday Discuss. **154**, 249 (2012).
[17]A. D. MacKerell, D. Bashford, M. Bellott, R. L. Dunbrack, J. D. Evanseck, M. J. Field, S. Fischer, J. Gao, H. Guo, S. Ha, D. Joseph-McCarthy, L. Kuchnir, K. Kuczera, F. T. Lau, C. Mattos, S. Michnick, T. Ngo, D. T. Nguyen, B. Prodhom, W. E. Reiher, B. Roux, M. Schlenkrich, J. C. Smith, R. Stote, J. Straub, M. Watanabe, J. Wiórkiewicz-Kuczera, D. Yin, and M. Karplus, J. Phys. Chem. B **102**, 3586 (1998).
[18]W. D. Cornell, P. Cieplak, C. I. Bayly, I. R. Gould, K. M. Merz, D. M. Ferguson, D. C. Spellmeyer, T. Fox, J. W. Caldwell, and P. A. Kollman, J. Am. Chem. Soc. **117**, 5179 (1995).
[19]W. L. Jorgensen, D. S. Maxwell, and J. Tirado-Rives, J. Am. Chem. Soc. **118**, 11225 (1996).
[20]C. Merlet, C. Péan, B. Rotenberg, P. A. Madden, P. Simon, and M. Salanne, J. Phys. Chem. Lett. **4**, 264 (2013).
[21]J. Vatamanu, O. Borodin, and G. D. Smith, J. Phys. Chem. B **115**, 3073 (2011).
[22]E. Paek, A. J. Pak, and G. S. Hwang, J. Electrochem. Soc. **160**, A1 (2013).

[23]E. Paek, A. J. Pak, K. E. Kweon, and G. S. Hwang, J. Phys. Chem. C **117**, 5610 (2013).
[24]A. J. Pak, E. Paek, and G. S. Hwang, Carbon **68**, 734 (2014).
[25]A. J. Pak, E. Paek, and G. S. Hwang, Phys. Chem. Chem. Phys. **15**, 19741 (2013).
[26]E. Paek, A. J. Pak, and G. S. Hwang, J. Phys. Chem. C **117**, 23539 (2013).
[27]B. C. Wood, T. Ogitsu, M. Otani, and J. Biener, J. Phys. Chem. C **118**, 4 (2014).
[28]G. Kaminski and W. L. Jorgensen, J. Phys. Chem. **100**, 18010 (1996).
[29]S. J. Plimpton, J. Comput. Phys. **117**, 1 (1995).
[30]See supplementary material http://dx.doi.org/10.1063/1.4905328 for additional discussion on equilibration procedures.
[31]W. G. Hoover, Phys. Rev. A **31**, 1695 (1985).
[32]U. Essmann, L. Perera, M. L. Berkowitz, T. Darden, H. Lee, and L. G. Pederson, J. Chem. Phys. **103**, 8577 (1995).
[33]I.-C. Yeh and M. L. Berkowitz, J. Chem. Phys. **111**, 3155 (1999).
[34]J. N. C. Lopes, J. Deschamps, and A. A. H. Pádua, J. Phys. Chem. B **108**, 2038 (2004).
[35]J. de Andrade, E. S. Böse, and H. Stassen, J. Phys. Chem. B **106**, 13344 (2002).
[36]L. Battezzati, C. Pisani, and F. Ricca, J. Chem. Soc., Faraday Trans. 2 **71**, 1629 (1975).
[37]J. P. Perdew, K. Burke, and M. Ernzerhof, Phys. Rev. Lett. **77**, 3865 (1996).
[38]S. Grimme, J. Comput. Chem. **27**, 1787 (2006).
[39]G. Kresse and J. Furthmüller, Phys. Rev. B **54**, 11169 (1996).
[40]H. J. Monkhorst and J. D. Pack, Phys. Rev. B **13**, 5188 (1976).
[41]S. Li, G. Feng, and P. T. Cummings, J. Phys.: Condens. Matter **26**, 284106 (2014).
[42]S. Zhang, N. Sun, X. He, X. Lu, and X. Zhang, J. Phys. Chem. Ref. Data **35**, 1475 (2006).
[43]To obtain the excess charge the spatial charge density of the graphene/IL system is subtracted by the individual spatial charge densities of the neutral graphene sheet, cations, and anions in the same atomic positions.
[44]J. Vatamanu, O. Borodin, D. Bedrov, and G. D. Smith, J. Phys. Chem. C **116**, 7940 (2012).
[45]M. Sha, Q. Dou, F. Luo, G. Zhu, and G. Wu, ACS Appl. Mater. Interfaces **6**, 12556 (2014).
[46]S. Wang, S. Li, Z. Cao, and T. Yan, J. Phys. Chem. C **114**, 990 (2010).
[47]S. Luryi, Appl. Phys. Lett. **52**, 501 (1988).
[48]L. A. Ponomarenko, R. Yang, R. V. Gorbachev, P. Blake, A. S. Mayorov, K. S. Novoselov, M. I. Katsnelson, and A. K. Geim, Phys. Rev. Lett. **105**, 136801 (2010).
[49]We should note that in our previous studies, the quantitative values for the DOS were mistakenly underestimated and have since been corrected.
[50]S. Das Sarma, S. Adam, E. Hwang, and E. Rossi, Rev. Mod. Phys. **83**, 407 (2011).
[51]Y. Lu, B. Goldsmith, D. R. Strachan, J. H. Lim, Z. Luo, and A. T. C. Johnson, Small **6**, 2748 (2010).